Electronic Supplementary Material (ESI) for Journal of Materials Chemistry A.

Supporting Information

for

The intrinsic mechanism of Co/Mn elemental manipulation in enhancing the cycling stability of single-crystal ultrahigh-Nickel layered cathode

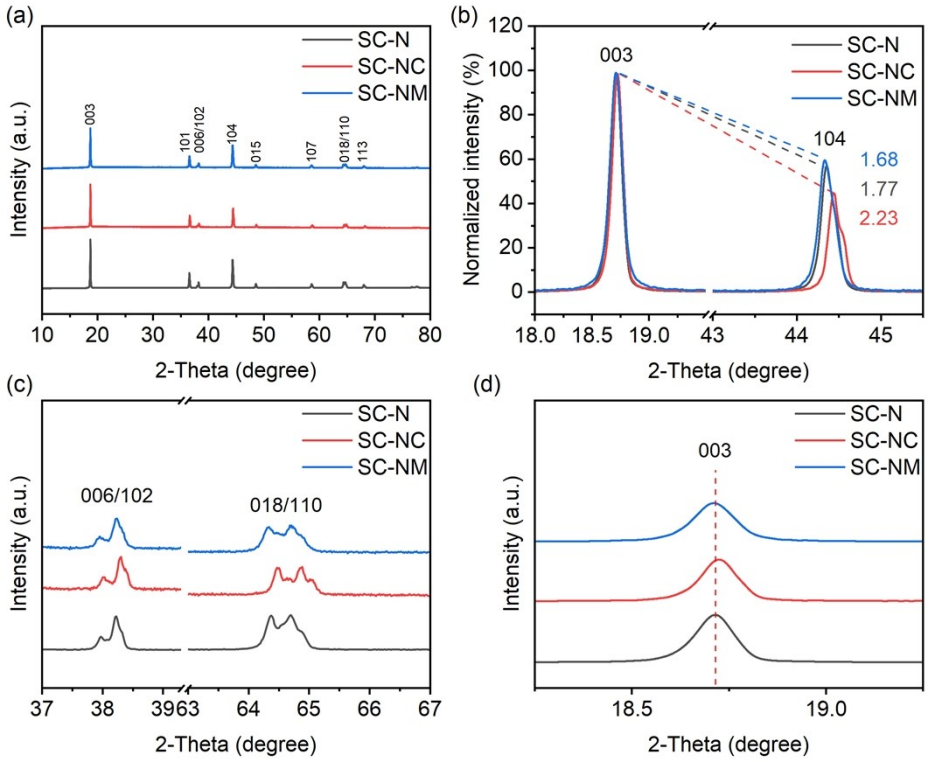

Fig. S1. (a) The comparison for XRD patterns of the SC-N, SC-NC and SC-NM samples. (b) The magnified patterns of 003 and 104 reflections with the calculated intensity ratios and (c) the magnified patterns of 006/102 and 018/110 splitting reflections. (d) The magnified patterns of 003 reflections to highlight the lattice parameter difference of the three cathodes.

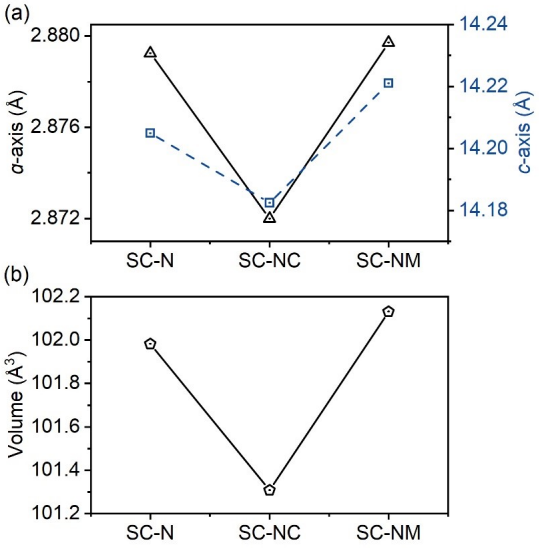

Fig. S2. Calculated (a) *a*- and *c*- lattice parameters and (b) unit cell volume of the synthesized SC-N, SC-NC, and SC-NM samples.

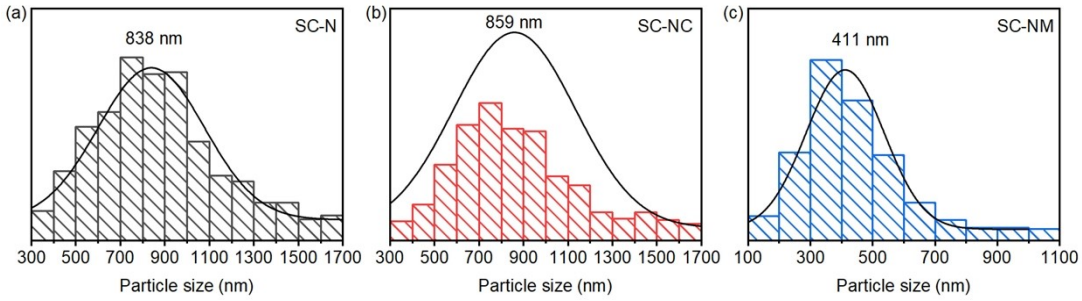

Fig. S3. The particle size distribution statistics and the corresponding D50 (median particle size) obtained from the SEM images of the (a) SC-N, (b) SC-NC, and (c) SC-NM samples.

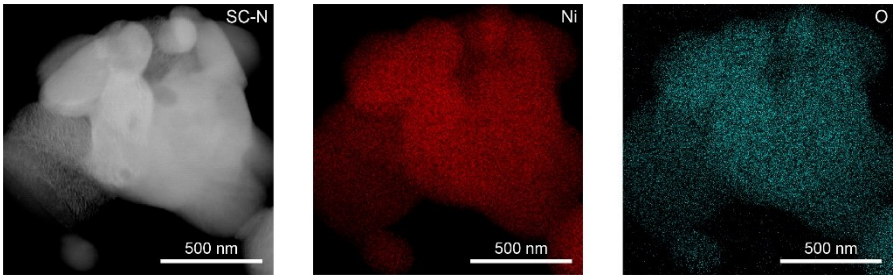

Fig. S4. The element distribution in TEM-EDS mapping of the SC-N sample.

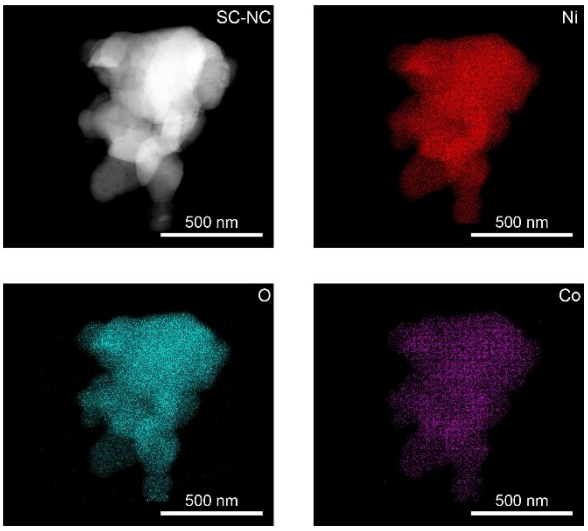

Fig. S5. The element distribution in TEM-EDS mapping of the SC-NC sample.

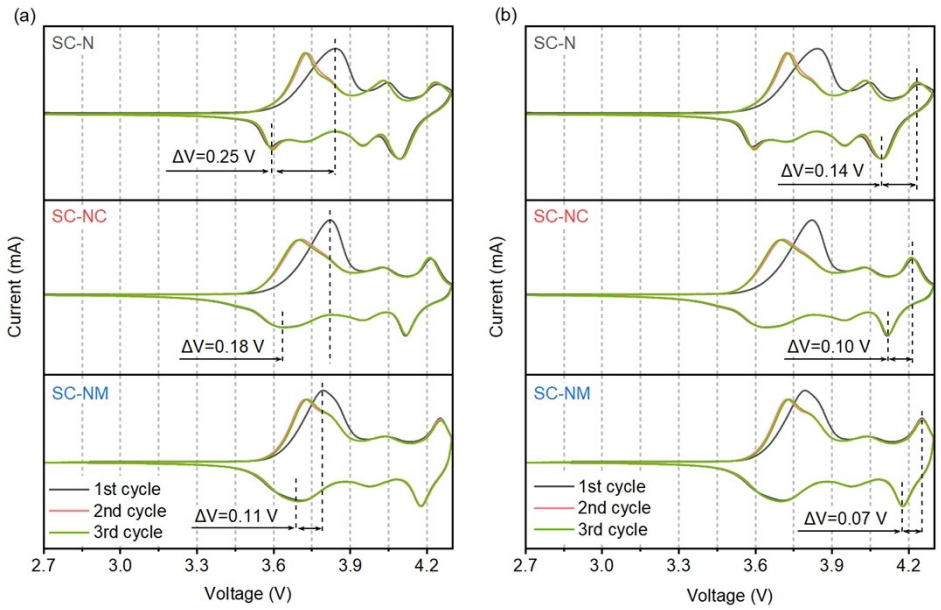

Fig. S6. CV profiles in the initial three cycles at scanning rate of 0.1 mV s^{-1} for the SC-N, SC-NC and SC-NM cathodes and the calculated overpotential between the redox peaks for (a) H1/M and (b) H2/H3 phase transition.

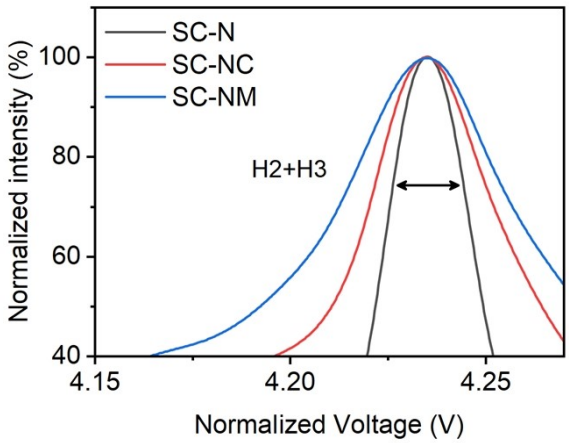

Fig. S7. Comparison of width of the H2/H3 phase transition peaks from the dQ dV^{-1} curves of the initial cycle of the cathodes.

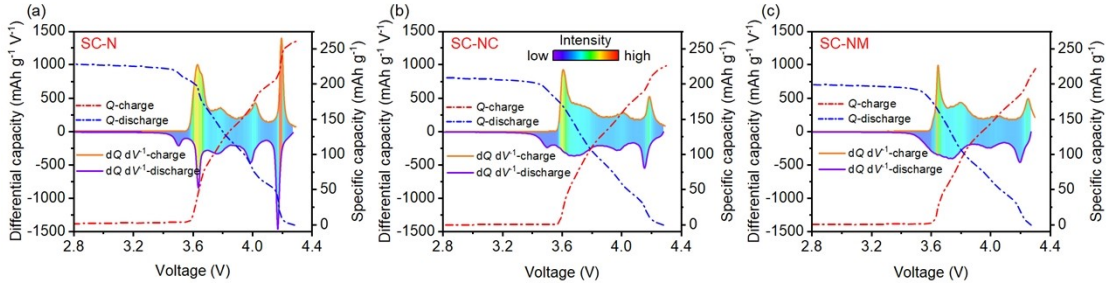

Fig. S8. The initial voltage-capacity curves and the dQ dV^{-1} curves of (a) SC-N, (b) SC-NC, and (c) SC-NM cathodes.

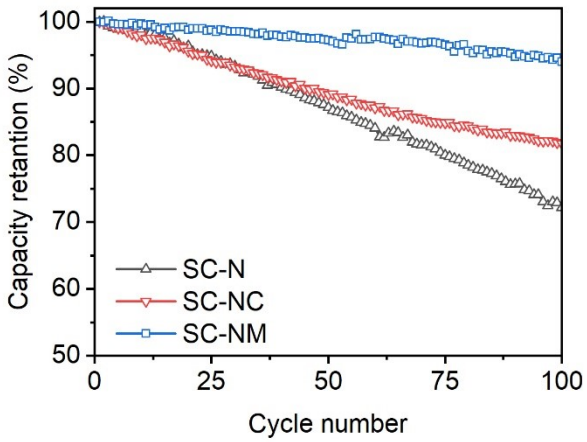

Fig. S9. Capacity retention of SC-N, SC-NC and SC-NM cathodes for 100 cycles at 0.5 C at the voltage range of 2.7 – 4.3 V.

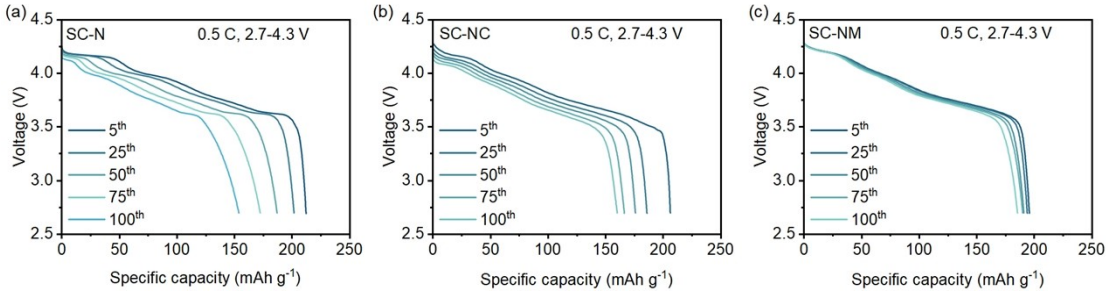

Fig. S10. The discharge curves at selected cycles of (a) SC-N, (b) SC-NC, and (c) SC-NM, respectively, at 0.5 C in the voltage range of 2.7-4.3 V.

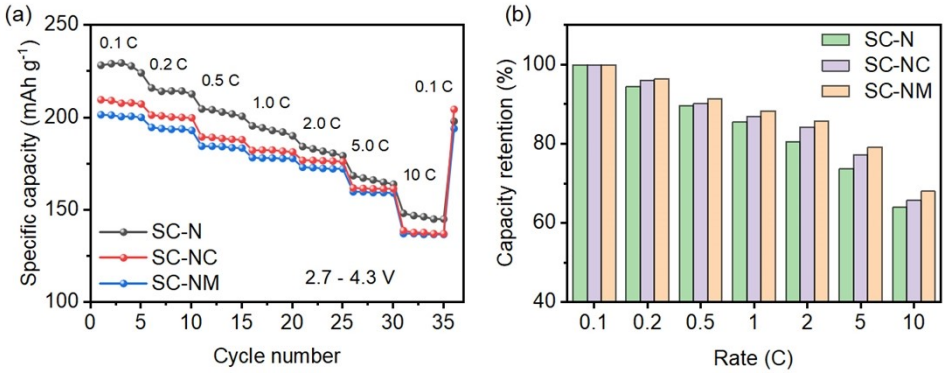

Fig. S11. The rate performance of single crystal cathodes between 2.7 and 4.3 V. (a) Discharge capabilities and (b) capacity retention ratio of the three cathode under different rate.

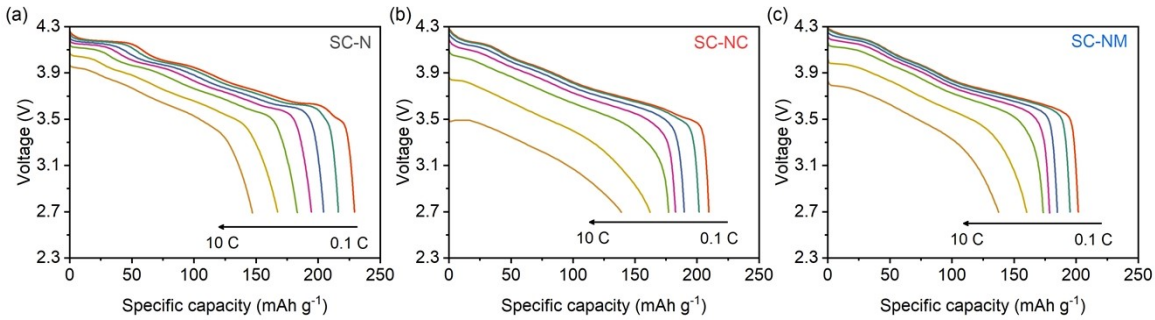

Fig. S12. Discharge capacity-voltage curves under different rates of (a) SC-N, (b) SC-NC, and (c) SC-NM.

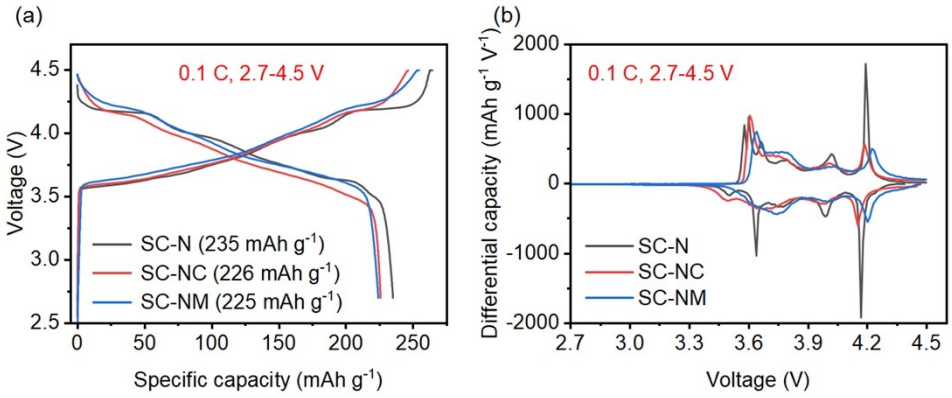

Fig. S13. (a) The initial charge/discharge profiles and (b) corresponding dQ dV^{-1} curves at 0.1 C rate of the SC-N, SC-NC and SC-NM cathodes.

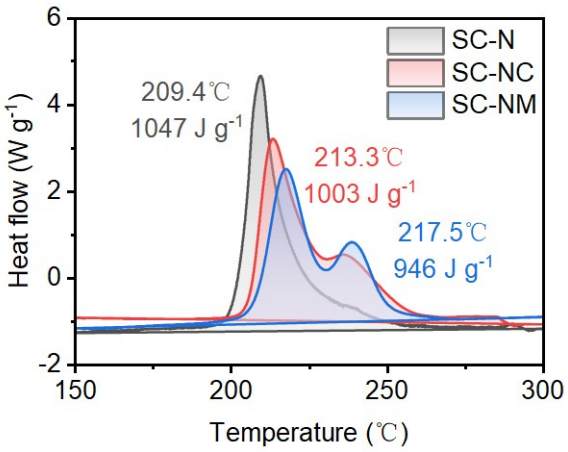

Fig. S14. The DSC profiles of the three cathodes under fully-charged state (4.3 V).

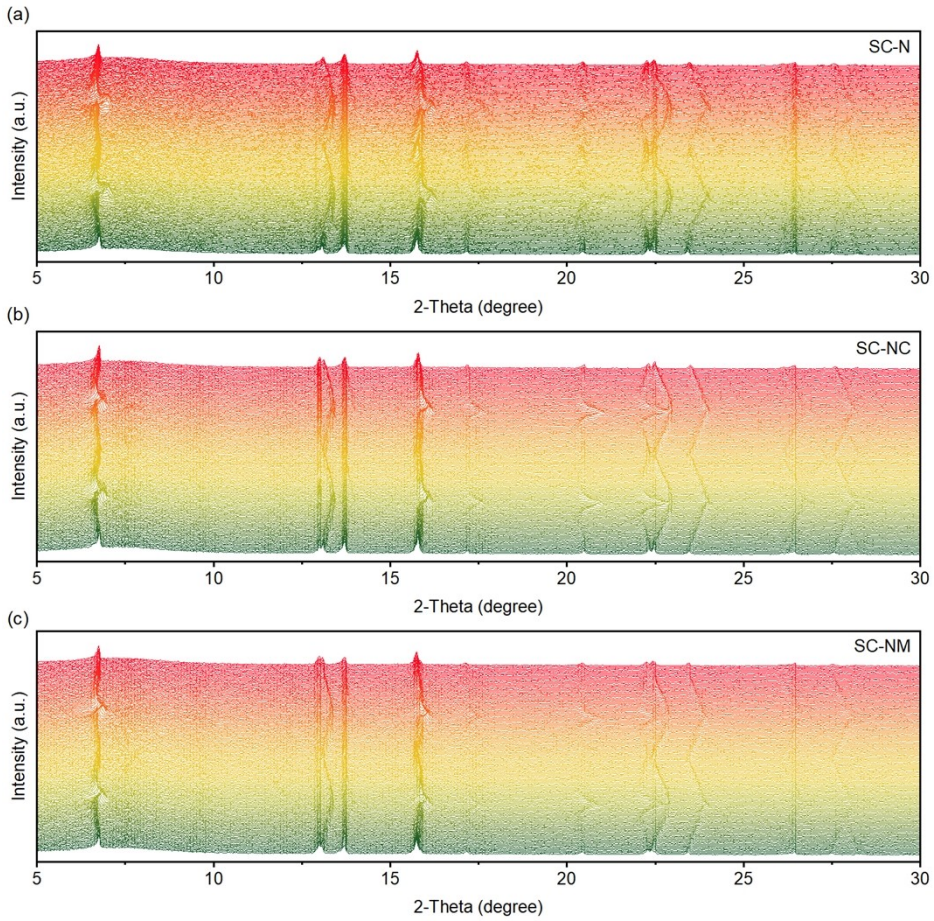

Fig. S15. Stacked profiles of the *in situ* XRD patterns of the (a) SC-N, (b) SC-NC, and (c) SC-NM cathode during the first two charge/discharge process.

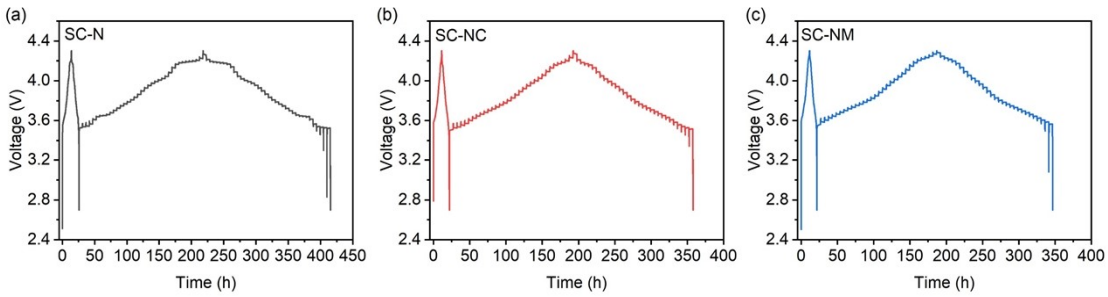

Fig. S16. Voltage-time curves obtained from the GITT tests of (a) SC-N, (b) SC-NC, and (c) SC-NM cathodes.

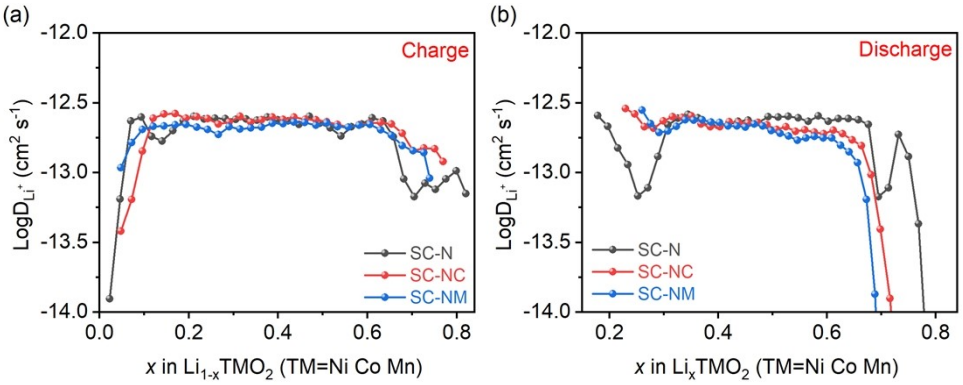

Fig. S17. The apparent Li^+ diffusion coefficient of the three cathodes as a function of state of charge or depth of discharge calculated from GITT test curves during (a) charge and (b) discharge process

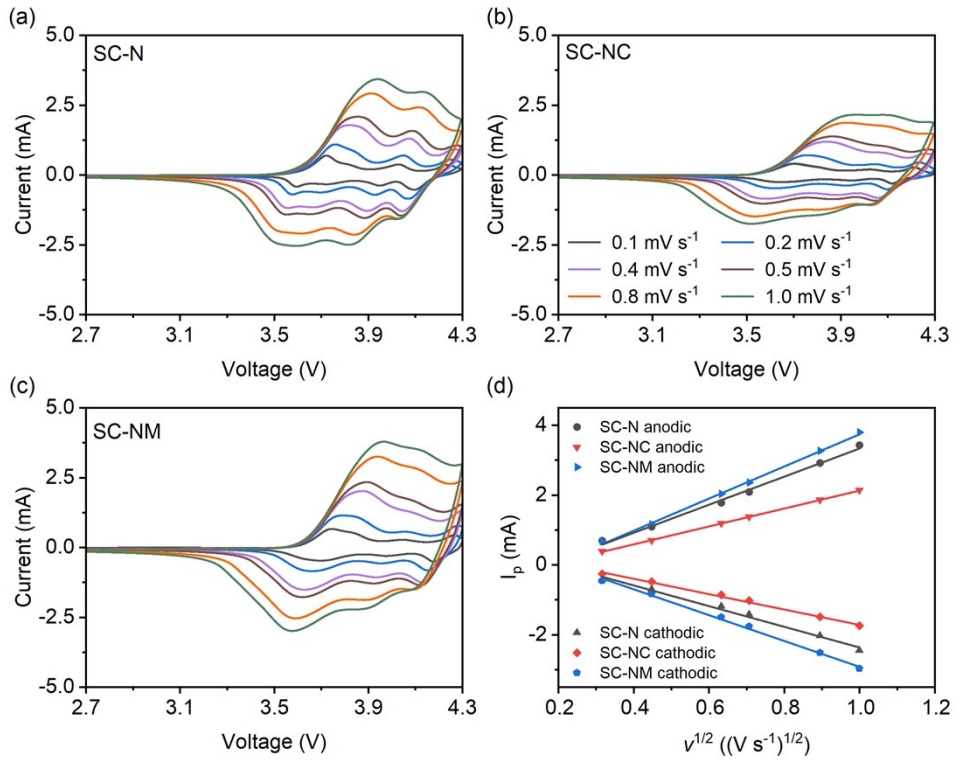

Fig. S18. CV profiles with different scanning rates between 2.7 and 4.3 V of (a) SC-N, (b) SC-NC, and (c) SC-NM cathodes. (d) The peak current during the charging and discharging process versus square root of scanning rate for the three cathodes.

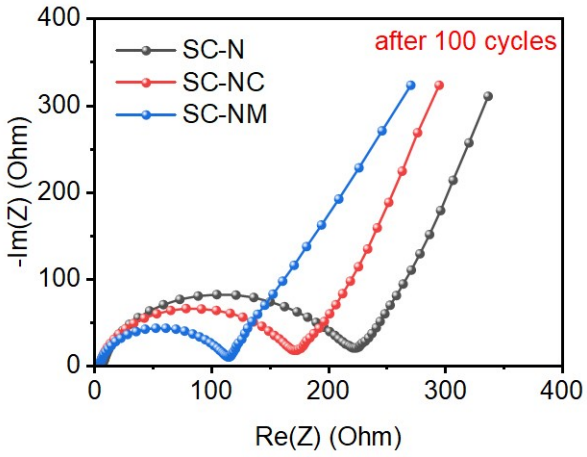

Fig. S19. EIS curves for three cathodes at full discharge state after 100 cycles.

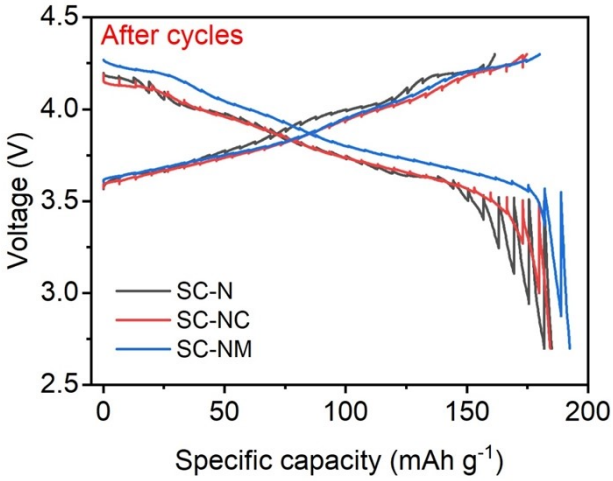

Fig. S20. Voltage-capacity curves obtained from the GITT tests for the three SC cathode after 100 cycles.

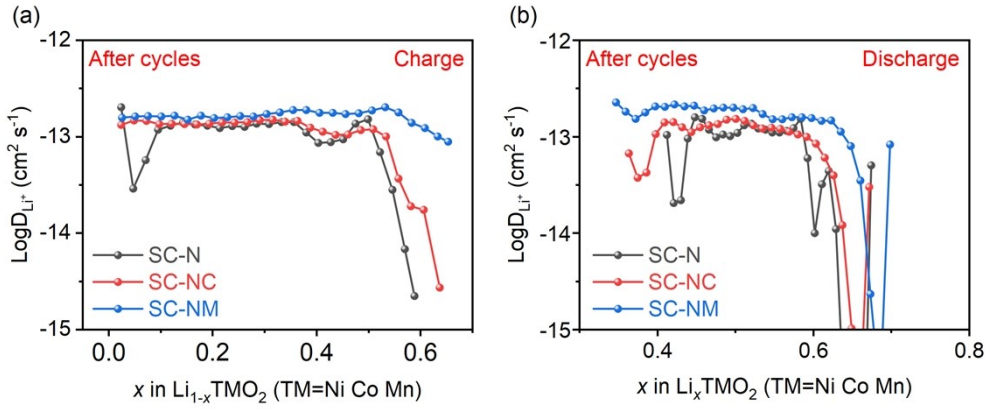

Fig. S21. Calculated Li^+ diffusion coefficient obtained from the GITT test curves of the

three cathodes after 100 cycles during the (a) charge and (b) discharge process.

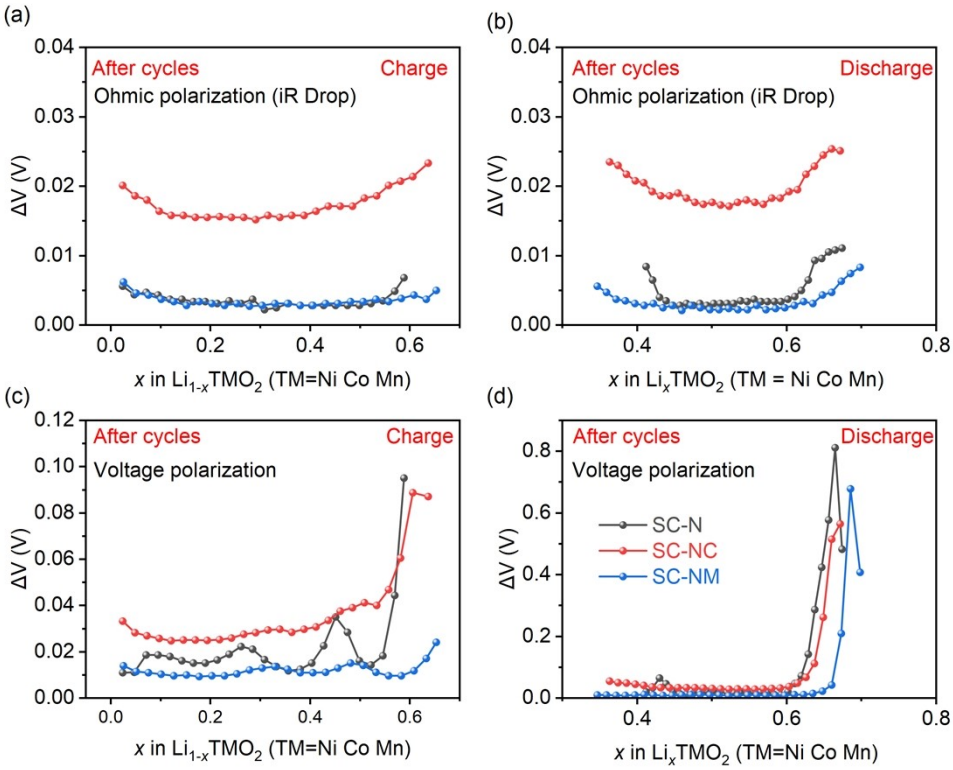

Fig. S22. The (a, b) ohmic polarization potential and (c, d) voltage polarization potential for the cycled cathodes during the charge and discharge process, respectively.

Table S1. Results of analysis by Inductively Coupled Plasma (ICP) of SC-N, SC-NC and SC-NM samples.

Samples	Li(mol%)	Ni(mol%)	Co(mol%)	Mn(mol%)
SC-N	49.91	50.09	/	/
SC-NC	50.07	45.04	4.89	/
SC-NM	50.03	44.98	/	4.99

Table S2. Lattice parameters of SC-N samples derived from the Rietveld refinement against the XRD patterns.

SC-N	Atom	Site	*x*	*y*	*z*	Occu.
a = 2.8792(5) Å	Li1	3a	0	0	0.0000	0.9639

c = 14.2049(2) Å	Ni1	3b	0	0	0.5000	0.9639
R_p = 11.1%	Li2	3b	0	0	0.5000	0.0362
R_{wp} = 7.51%	Ni2	3a	0	0	0.0000	0.0362
Chi^2 = 7.33	O	6c	0	0	0.2446	1

Table S3. Lattice parameters of SC-NC samples derived from the Rietveld refinement against the XRD patterns.

SC-NC	**Atom**	**Site**	***x***	***y***	***z***	**Occu.**
a = 2.8720(0) Å c = 14.1823(8) Å R_p = 7.8% R_{wp} = 10.8% Chi^2 = 1.63	Li1	3a	0	0	0.0000	0.9808
	Ni1	3b	0	0	0.5000	0.8807
	Li2	3b	0	0	0.5000	0.0192
	Ni2	3a	0	0	0.0000	0.0192
	Co	3b	0	0	0.5000	0.0999
	O	6c	0	0	0.2446	1

Table S4. Lattice parameters of SC-NM samples derived from the Rietveld refinement against the XRD patterns.

SC-NM	**Atom**	**Site**	***x***	***y***	***z***	**Occu.**
a = 2.8797(2) Å c = 14.2210(0) Å R_p = 7.5% R_{wp} = 11.2% Chi^2 = 3.34	Li1	3a	0	0	0.0000	0.9500
	Ni1	3b	0	0	0.5000	0.8460
	Li2	3b	0	0	0.5000	0.0540
	Ni2	3a	0	0	0.0000	0.0540
	Mn	3b	0	0	0.5000	0.0999
	O	6c	0	0	0.2446	1

Table S5. Lattice parameters before and after 100 cycles of SC-N, SC-NC, and SC-NM cathodes obtained from Rietveld refinement against XRD patterns.

Samples	*a* (Å)	*c* (Å)	*V* (Å^3)
SC-N (before cycle)	2.8792(5)	14.2049(2)	101.9830
SC-N (after cycle)	2.8695(6)	14.2599(0)	101.6762
SC-NC (before cycle)	2.8720(0)	14.1823(8)	101.3091
SC-NC (after cycle)	2.8617(0)	14.2370(0)	100.9762
SC-NM (before cycle)	2.8797(2)	14.2210(0)	102.1319
SC-NM (after cycle)	2.8726(6)	14.2745(2)	102.0068